CrossMark

ORIGINAL ARTICLE

A new method to approximate load–displacement relationships of spinal motion segments for patient-specific multi-body models of scoliotic spine

Athena Jalalian[1] · Francis E. H. Tay[1] · Soheil Arastehfar[1] · Gabriel Liu[2]

Abstract Load–displacement relationships of spinal motion segments are crucial factors in characterizing the stiffness of scoliotic spine models to mimic the spine responses to loads. Although nonlinear approach to approximation of the relationships can be superior to linear ones, little mention has been made to deriving personalized nonlinear load–displacement relationships in previous studies. A method is developed for nonlinear approximation of load–displacement relationships of spinal motion segments to assist characterizing in vivo the stiffness of spine models. We propose approximation by tangent functions and focus on rotational displacements in lateral direction. The tangent functions are characterized using lateral bending test. A multi-body model was characterized to 18 patients and utilized to simulate four spine positions; right bending, left bending, neutral, and traction. The same was done using linear functions to assess the performance of the proposed tangent function in comparison with the linear function. Root-mean-square error (RMSE) of the displacements estimated by the tangent functions was 44 % smaller than the linear functions. This shows the ability of our tangent function in approximation of the relationships for a range of infinitesimal to large displacements involved in the spine movement to the four positions. In addition, the models based on the tangent functions yielded 67, 55, and 39 % smaller RMSEs of Ferguson angles, locations of vertebrae, and orientations of vertebrae, respectively, implying better estimates of spine responses to loads. Overall, it can be concluded that our method for approximating load–displacement relationships of spinal motion segments can offer good estimates of scoliotic spine stiffness.

Keywords Scoliosis · Spine stiffness · Spinal motion segment · Nonlinear load–displacement relationship · Patient-specific multi-body model

1 Introduction

Scoliosis is a complex three-dimensional (3D) structural deformity of the human spine, which often requires surgery for correction of severe deformities [13]. To assist surgeons with planning scoliosis surgery, multi-body models of scoliotic spine are effectively helpful because they can provide predictive information about the surgery outcome [18, 22]. For the models to become more reliable tools for prediction of the surgery, one essential step is in vivo characterization of the stiffness of the spine models as scoliosis is a very patient-specific deformity [19, 32]. Such personalization can have significant effects on the accuracy of the models to simulate the spine responses to loads [32]. One of the mechanical properties, crucial for characterizing the spine stiffness, is the load–displacement relationships of the spinal motion segments [25]. These relationships play important roles in determining the rotational and translational displacements of vertebrae with respect to their inferior vertebrae against the loads and thus in determining the model responses to loads. To define the load–displacement relationships, Panjabi pioneered the concept of 6×6 stiffness matrices [29]. Aubin et al. [4] introduced it to the multi-body modelling of the scoliotic spine. Following this,

✉ Athena Jalalian
athena@u.nus.edu

[1] Department of Mechanical Engineering, Block EA, #02-17, National University of Singapore, 1 Engineering Drive 2, Singapore 117576, Singapore

[2] Department of Orthopedic Surgery, National University of Singapore, Singapore, Singapore

Springer

Petit et al. [32] derived an algorithm based on the lateral bending test to personalize the stiffness coefficients (elements of the 6 × 6 stiffness matrices) and showed improvements in the model responses to loads.

The stiffness matrices have been mainly defined according to Hooke's law, which is a linear approximation to the responses of motion segments to loads [34]. The stiffness coefficients are most commonly estimated for infinitesimal displacement of a vertebra with respect to its inferior vertebra [9, 26, 37]. However, the displacements featured in vertebral motions are often *finite* [27, 36]. Besides, referring to the experimental studies done on the displacements of vertebrae against the loads [16, 29, 30, 39], the change of the displacements of vertebrae significantly reduces when the load increases. This implies that the linear approximations made according to the infinitesimal displacements result in overestimation of the displacements of vertebrae, showing underestimation of stiffness of spinal motion segments. To tackle this issue, O'Reilly et al. [27] studied linear approximations made based on the finite displacements against the loads. However, the linear approximation, made based on either infinitesimal or finite displacements, is far from the nonlinear nature of load–displacement behaviour of spinal motion segments [34], according to the experimental data [3, 15]. In addition, the linear approximations cannot offer the bounded displacements, which is an important characteristic of the elastic behaviour of motion segments [16, 30]. The unbounded displacements resulted from the linear approximations can negatively affect the accuracy of simulations of the typical spine positions such as lateral bending and flexion/extension positions, in which the displacements of the vertebrae are generally close to their bounds. This can cause problems for the personalization methods based on the lateral bending test that involves the simulation of the lateral bending positions. Besides, in the surgery simulation, the spine models with the patient-specific Hookean (linear elastic) motion segments may suffer from excessive and unbounded displacements of the vertebrae in the presence of the large forces and moments exerted on the fused vertebrae [5, 35]. Overall, the suitability of utilizing the Hooke's law to characterization of the load–displacement behaviour of spinal motion segments is questionable, especially in the applications involving large loads. Thus, the assumption of the linear elastic motion segments needs to be revised [34].

To overcome these complications, Abouhossein et al. [1] defined nonlinear responses for the spinal motion segments as a series of nonlinear B-splines fitted to in vitro load–displacement curves obtained experimentally by Heuer et al. [16]. Besides, Rupp et al. [34] and Huynh et al. [17] used polynomials to approximate the responses to loads. Nevertheless, these studies were on intact spine. Besides, they did not contribute towards personalization

of the nonlinear relationships. Although the nonlinear approach to approximation of the load–displacement relationships can be superior to the linear approaches in characterizing the spine stiffness [34, 36, 39], study on deriving the patient-specific nonlinear load–displacement relationships of spinal motion segments for scoliotic spine models is considerably lacking in the existing literature. Therefore, this paper aims to develop a method for nonlinear approximation of the load–displacement relationships of spinal motion segments to assist characterizing in vivo the stiffness of the scoliotic spine models. In this study, we focus on the rotational responses of the motion segments in the lateral direction, and the load is the moment about the intervertebral discs of the motion segments. Our scope is narrowed to adolescent idiopathic scoliosis (AIS) that affects 2–3 % of adolescents [7] and mostly occurs in females [2, 23].

2 Methods

First, we propose a nonlinear function to approximate the load–displacement relationships of the spinal motion segments, and then, we characterize the function for individual motion segments by using lateral bending test [19, 22, 24] to develop patient-specific scoliosis spine models. To study the approximation, the rotational displacement (r) of the motion segments is measured. r of a motion segment pertains to the amount of rotation of the superior vertebra with respect to the inferior vertebra during the spine movement from the erect[1] to a position. According to lateral bending test [24, 33], r is obtained by using orientations (Θ) of the vertebrae measured on the pre-operative X-rays of posterior-anterior positions in the coronal plane (erect, right bending, and left bending).

Second, we determine whether the patient-specific spine models developed based on the proposed nonlinear function can possess the stiffness of scoliosis spines. As the stiffness determines the displacement responses to loads, one factor that can show how well the stiffness is estimated is the spine shape. Thus, we study the accuracy of the patient-specific spine models to reconstruct the spine shape in different spine positions; the more accurate shapes can imply the better estimates of the stiffness. In this study, the developed patient-specific spine models are used to simulate four spine positions (left bending, right bending, neutral, and traction) for which the X-rays were available. Then, the accuracy is tested by using estimation errors of

---

[1] The erect position is considered as the resting position of the spine in scoliotic spine models, i.e. it is assumed that there is no load on the spine model and r of all vertebrae is zero [5, 21, 32].

Table 1 Descriptive data of the patients

Patient	Gender	Age (year)	Lenke classification	Cobb angle (°) of the main curve
1	Female	13	1A	49
2	Female	15	1B	53
3	Female	16	1C	46
4	Female	12	1C	48
5	Female	13	2A	53
6	Female	16	2B	53
7	Female	19	2C	48
8	Female	14	2C	55
9	Female	15	3A	59
10	Female	13	4C	86
11	Female	12	5C	62
12	Female	14	6C	59
13	Male	14	2A	59
14	Male	19	2B	48
15	Male	18	2B	61
16	Male	18	3B	46
17	Male	14	3C	53
18	Male	19	3C	70

Ferguson angles [5, 32] and the locations (LOC) [19, 20] and Θ of the vertebrae [20]. These errors can show how well the spine curvature is reproduced and how well the vertebrae are placed along the spine.

2.1 Subjects and data collection

The current study has been approved by the domain specific review board (DSRB) and ethics committee. All the patients involved had been properly consulted, and their approval and informed consents were obtained. Following the DSRB approval and obtaining the proper informed consents, the five pre-operative digital X-rays of 18 patients with AIS were used for the study (Table 1). The patients had no neurological deterioration, and they were admitted to hospital for surgical treatment. There were 12 female patients and six male patients between the ages of 12 and 19 years (mean age of 15 years). Cobb angle of the main curves ranged from 46° to 86°, and the average and median Cobb angles were 56° and 53°, respectively.

The digital X-rays were analysed to measure LOC and Θ of the vertebrae from L4 to T2 to obtain the spine curvatures in the five positions. L5 and T1 were not included since the X-rays obtained at these vertebrae were often suboptimal for measurement of LOC and Θ. The X-rays had pixels with size of 0.1×0.1 mm^2. LOC was defined as the location of the mid-point of the vertebral body in the coronal plane (Fig. 1). The mid-point is the intersection of the line drawn from the upper left corner to the lower right of the vertebral body and the line drawn from the upper right to the lower left of the vertebral body [40]. To find the
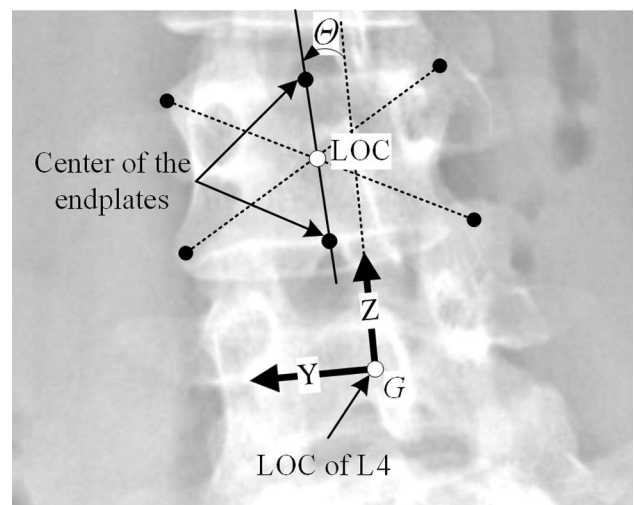

Fig. 1 Illustration of the global coordinate system on L4, and illustration of LOC and Θ on L3

mid-points, landmarks were manually selected at the four corners of the vertebral body. A landmark was a pixel of the X-rays. Θ was considered as the orientation of the line (Fig. 1) passing through the centre of the upper and lower endplates of the vertebra (in accordance with the definition of *vertebral lateral rotation* [38] provided by Scoliosis Research Society). For Θ, after localizing the mid-point of a vertebra, a line coincident with the mid-point is drawn on the X-ray. This line was manually rotated about the mid-point until it shows the orientation. The step of the rotation was 0.1°. LOC and Θ were defined in the global

coordinate system (*G* in Fig. 1) represented by *XYZ* on L4. *G* has its origin at the mid-point of L4. *X*- and *Y*-axes define the anterior and left directions. *Z*-axis is parallel to the line that shows the orientation of L4. The plane *YZ* is the coronal plane, and LOC is given by the ordered pair of (*Y, Z*). According to the definition of *G*, LOC and *Θ* of L4 are (0, 0) mm and 0°, respectively. MATLAB R2013b version 8.2.0.701 (MathWorks, Natick, MA, USA) was used for the analyses of the X-rays.

Two experts familiar with X-rays of the spine performed the measurements of LOC and *Θ* three times. Then, the mean values of the measurements were considered. All the measurements were supervised by G. Liu (one of the authors) who is an experienced scoliosis surgeon at National University Hospital, Singapore. The intra- and inter-observer reliabilities of the measurements were evaluated by using Pearson correlation analysis. The intra-observer reliabilities of the measurements were 0.95 ± 0.03 for expert one and 0.92 ± 0.02 for expert two. The inter-observer coefficient was 0.90. These agreements are excellent according to [11] and demonstrate the repeatability and reliability of the measurements.

2.2 Nonlinear approximation of load–displacement relationships

Load–displacement curves of motion segments during lateral bending movements in the coronal plane possess three fundamental characteristics by referring to the experimental data reported in the literature [16, 28, 30]. In a spinal motion segment:

1. Rotational displacement of the superior vertebra from its resting position is zero if and only if the moment about the intervertebral disc (*τ*) is zero [30].
2. When the moment increases, the change (Δ) of the rotational displacement significantly reduces [16, 39], i.e. if $\tau \to \pm\infty$, then $\Delta r \to 0$.
3. The rotational displacement is limited [16]. When the moment is approaching $\pm\infty$, the displacement reaches a limited value.

According to the abovementioned characteristics, we propose that the load–displacement relationships in the coronal plane can be approximated by a tangent function as expressed in (1).

$$\tau = A \cdot (\tan(B \cdot r + C) + D), \quad -\frac{\pi}{2} \leq B \cdot r + C \leq \frac{\pi}{2} \quad (1)$$

The parameters *A, B, C,* and *D* in (1) modify the tangent function to approximate the load–displacement relationship for individual motion segments (Fig. 2). *A* stretches the tangent function along *τ*-axis to vary the stiffness. *B*
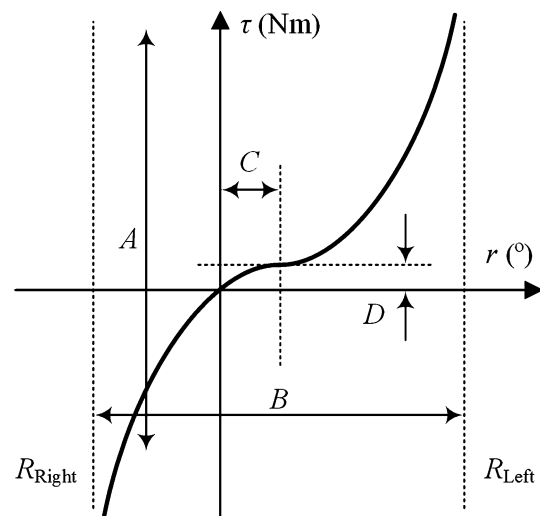

Fig. 2 The parameters to modify the proposed tangent function to approximate the load–displacement relationship of a spinal motion segment

stretches the tangent function along *r*-axis to allow the representation of different range of motion of the vertebrae. *C* is introduced to translate the tangent function along *r*-axis because the range of motion of vertebrae may not be equal in the right and left bending movement [14, 41]. *D* eliminates the bias along *τ*-axis so that the zero *τ* results in the zero *r* (the first characteristic).

2.3 Characterizing the load–displacement relationships for individual spinal motion segments

For a spinal motion segment:

First, the two asymptotes of the tangent function are estimated. They are the largest lateral rotation of a vertebra towards the right and left sides, represented by R_{Right} and R_{Left} (Fig. 2). $R_{Right/Left}$ is estimated by $1.2 \times r_{Right/Left}$. We use $r_{Right/Left}$ for estimation of the asymptotes because the bending X-rays are taken while the patients perform maximum voluntary bending movements to the right and left sides, implying that there may be small differences between $R_{Right/Left}$ and $r_{Right/Left}$. The reason for 1.2 (20 %) enlargement of the range of *r* is explained in "Appendix". According to our previous study [22], a number of vertebrae in a scoliotic spine may not rotate in the direction of the bending movement. In this case, the maximum *r* of left and right bending is considered for both R_{Right} and R_{Left}, i.e. $R_{Right} = -1.2 \times \max(|r_{Right}|, |r_{Left}|)$ and $R_{Left} = 1.2 \times \max(|r_{Right}|, |r_{Left}|)$; note that the rotations towards the right side (i.e. clockwise) are negative.

Second, the values of *B* and *C* are calculated by using (2). Equation 2 is a set of two linear equations derived by using $R_{Right/Left}$ and the range of $B \cdot r + C$ in (1).

$$\begin{cases} B \cdot R_{\text{Right}} + C = -\frac{\pi}{2} \\ B \cdot R_{\text{Left}} + C = \frac{\pi}{2} \end{cases} \rightarrow \begin{cases} B = \frac{\pi}{R_{\text{Left}} - R_{\text{Right}}} \\ C = -\frac{\pi(R_{\text{Left}} + R_{\text{Right}})}{2(R_{\text{Left}} - R_{\text{Right}})} \end{cases} \quad (2)$$

Third, D is given by (3) according to the first characteristic.

$$D = -\tan(C) \quad (3)$$

Fourth, A is obtained by using the linear regression method and the load–displacement data, i.e. the pairs of (r, τ), as expressed in (4).

$$A = \frac{\left|f_{\text{Right}}\right| \cdot d_{\text{Right}}(\tan(B \cdot r_{\text{Right}} + C) + D) + \left|f_{\text{Left}}\right| \cdot d_{\text{Left}}(\tan(B \cdot r_{\text{Left}} + C) + D)}{(\tan(B \cdot r_{\text{Right}} + C) + D)^2 + (\tan(B \cdot r_{\text{Left}} + C) + D)^2} \quad (4)$$

where, $|\cdot|$ denotes the magnitude. f is the force[2] exerted on the spine to simulate the bending positions, and d is the moment arm of f about the joints of motion segments.

To set the value of A, the minimization problem expressed in (5) is defined.

$$\begin{aligned} &\text{minimize} \sum_{i=1}^{14} \text{RMSE}_i \\ &\text{subject to constraint} \quad 0 < \left|f_{\text{Right}}\right| \cdot d_{\text{apex,Right}} \\ &\quad, \left|f_{\text{Left}}\right| \cdot d_{\text{apex,Left}} < 63 \text{ N m} \end{aligned} \quad (5)$$

where, RMSE_i is the RMSE between the identified tangent function and the load–displacement data for ith motion segment; $i = 1$ to 14 correspond to the motion segments from L3–L4 to T2–T3. d_{apex} is the moment arm about the intervertebral disc of the apical vertebra in the thoracolumbar/lumbar region.

This minimization problem was defined to identify A, because in vivo measurement of the magnitudes of f for solving (4) may not be practically possible [6, 36]. Besides, the magnitude of f is a very patient-specific parameter depending on the spine stiffness. The minimization problem looks for $(f_{\text{Right}}, f_{\text{Left}})$ in the defined 2D domain of $|f_{\text{Right}}| \times |f_{\text{Left}}|$ so that the resulting A for the motion segments (4) provides the tangent functions that best fit the pairs of $(r, \tau) = (r_{\text{Right/Left}}, |f_{\text{Right/Left}}| \cdot d_{\text{Right/Left}})$.

The upper bound of the moment in (5) was proposed as the minimum value for the upper bound to reduce the computational costs of the minimization problem; in general, (5) can be solved with the upper bound of ∞. The upper bound was set based on Petit et al.'s [32] measurements of the intervertebral moments. The measured moment about the intervertebral discs of the apical vertebrae in the thoracolumbar/lumbar region had the highest value. According

to the reported mean and SD of this moment and Chebyshev's theorem, the range of [0, 63] Nm can cover 99 % of the moment population exerted on the intervertebral discs, implying that 63 Nm can be a good choice for the upper bound in (5).

2.4 Proof of concept

For each patient in our cohort of 18, the tangent function was characterized for individual spinal motion segments, and incorporated into a multi-body model of scoliotic spine. The models were then utilized to simulate the spine in four positions: right bending, left bending, neutral, and traction positions. To evaluate the success in estimating the spine stiffness by the proposed tangent function, the same was done by using the linear approach, and the simulation results were compared. For the linear approach, the stiffness coefficients were characterized in vivo by using Petit et al.'s personalization method [32]. Thus, two patient-specific models were created for each patient, namely Model-1 based on the tangent functions and Model-2 based on the linear functions.

The success in approximation of the load–displacement relationships was assessed by testing the accuracy of the estimates of r in the abovementioned four positions; RMSE of r (E_r) was calculated. The spine movement from the erect (resting position, footnote 1) to these four positions involves a range of displacements from infinitesimal to large displacements, and this can challenge the ability of the functions to approximate the load–displacement relationships.

To evaluate the success in estimating the spine stiffness, the accuracy of the simulations in the four positions was tested. To do this, we calculated RMSEs between the measured and estimated Ferguson angles according to [12, 32], and RMSEs of LOC (E_{LOC}) and Θ (E_Θ) according to [20]. E_{LOC} was calculated as Euclidian distance between LOC given by the models and those measured on the X-rays. E_{LOC} and E_Θ demonstrate how accurately the models place the vertebrae at their measured locations and orientations along the spine column. Thus, such RMSEs can show the degree to which the simulated spines fit the patients' spine in a position and therefore can imply how well the spine stiffness is estimated. RMSEs were calculated in the coronal plane because the X-rays, as the gold standard for the measurement of Ferguson angles, LOC, and Θ [31, 43], were available only in the coronal plane for the four positions.

---

[2] In multi-body models of the scoliotic spine, to simulate the lateral bending positions, a force is typically exerted on the uppermost vertebra in the spine model in the erect position [12].

The scoliotic spine model in this study was closest in similarity to the model in Petit et al.'s study. The initial 3D geometry of the model was personalized to the patients by using 2D X-rays according to 3D reconstruction method of Cheriet et al.'s [8]. Vertebrae were considered as rigid bodies [1, 42]. The intervertebral discs were defined as articulated mechanisms with a spherical joint allowing 3-DOF in rotation [10]. The spherical joints were placed at the posterior extremity of the superior endplate of each vertebra [32]. The relative translations between the vertebrae in a functional spinal unit were constrained according to [29]. Linear torsion springs were incorporated into the mechanism for DOFs of the vertebral axial rotation and vertebral flexion/extension [28]. For the DOF allowing the lateral rotation, the torsion springs were characterized by the proposed tangent function (nonlinear torsion springs) in Model-1 and by the constant stiffness coefficients (linear torsion springs) in Model-2.

To simulate the spine positions, translational and rotational displacements were imposed to the uppermost vertebra (T2) until its measured location (Y and Z) and orientation (Θ) were reproduced. The simulated spines were obtained by solving the equilibrium equations ($\sum f = 0$, $\sum \tau = 0$) since the spines were in static equilibrium (i.e. the spine elements were not moving) in the positions. Simulations were performed by using Robotics Toolbox version 9.10 (released on 24 February 2015) in MATLAB R2013b version 8.2.0.701 (MathWorks, Natick, MA, USA).

3 Results

3.1 Assessment of the approximated load–displacement relationships

E_r of 504 displacements[3] estimated by Model-1 and Model-2 in the bending positions was 1.44° and 2.59°, respectively, showing 44 % more accurate estimates of r by our nonlinear approach compared to the linear approach. As the rotational displacements are generally close to their boundary limits in the lateral bending positions,[4] the smaller RMSE by Model-1 implies that the proposed tangent function can make better approximation of the load–displacement relationships when the displacements are close to their limits; more than $0.8R_{\text{Right/Left}}$ in this study. This can be attributed to the significant

---

[3] 504 displacements = 14 vertebrae from L3 to T2 × 2 positions × 18 patients; note that L4 had no displacement according to definition of G.

[4] The bending X-rays are taken while the patients perform maximum voluntary bending movements to the right/left sides, implying small difference between R and r.
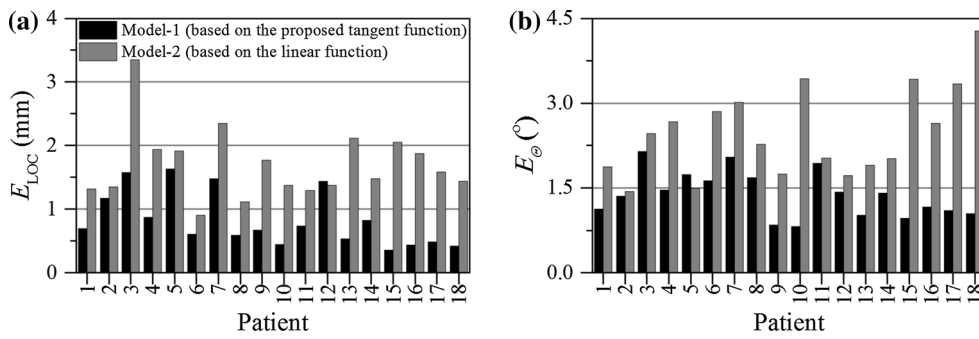
reduction in $\Delta r/\Delta \tau$ (characteristic 2, Sect. 2.2) and the bounded displacements (characteristic 3, Sect. 2.2) offered by the tangent function to suppress the excessive displacements. For the neutral and traction positions not included in the characterization of the tangent functions, E_r of 504 displacements was 1.30° by Model-1 and 2.15° by Model-2. An analysis of the displacements in these positions showed that around 77 % of the vertebrae rotated less than $0.8R_{\text{Right/Left}}$, implying that the rotational displacements were finite and/or infinitesimal. Thus, the smaller E_r (40 %) by Model-1 demonstrates that the proposed tangent functions can also make better approximation of the load–displacement relationships compared to the linear functions when the displacements are finite and/or infinitesimal. According to these results, it can be concluded that the proposed tangent function can outperform the linear functions in approximation of the load–displacement relationships.

3.2 Assessment of the estimated spine stiffness

For Model-1 based on the proposed tangent function, RMSE of Ferguson angles was 1° in the lateral bending positions. This RMSE is considered small according to the acceptable errors (less than 5° in [5, 25, 33]) reported in the literature. For Model-2 based on the linear function, RMSE of Ferguson angles was 3°, 3 times greater than the RMSE obtained by Model-1. It is worth mentioning that even though characterization of the stiffness of Model-2 involved minimization of estimation errors of Ferguson angles (see [32]), Model-1 characterized by our method (not considering the Ferguson angles for the characterization) was more successful in estimation of these regional angles. In addition, E_{LOC} and E_{Θ} by Model-1 were averagely 55 and 39 % smaller than the errors by Model-2, respectively (Figs. 3, 4). Therefore, Model-1 could be more successful in estimating the spine response to loads and placing the vertebrae at their respective locations and orientations along the spine, in comparison with Model-2. Overall, we showed the potential capability of the proposed tangent function over the linear functions for characterization of the spine stiffness.

Model-1 resulted in E_{LOC} of 0.83 ± 0.42 mm and E_{Θ} of $1.38 \pm 0.39°$ in the bending positions (Fig. 3). E_{LOC} and E_{Θ} in the neutral and traction positions were 0.75 ± 0.33 mm and $1.25 \pm 0.37°$, respectively (Fig. 4). These RMSEs can show that Model-1 could simulate the spine positions not included in the characterization of the tangent functions as accurate as the bending positions. Therefore, it can be concluded that our method for approximating the load–displacement relationships is able to provide good estimates of the scoliotic spine stiffness.

Fig. 3 RMSEs for the positions included in the personalization for each patient, **a** E_{LOC} and **b** E_{Θ}
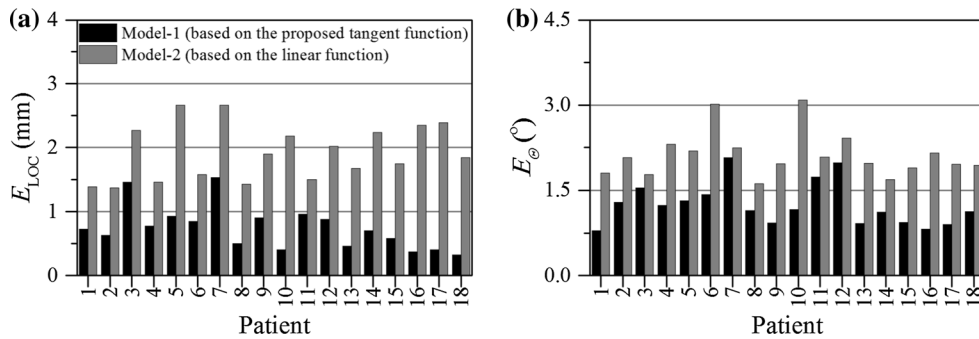

Fig. 4 RMSEs for the positions not included in the personalization for each patient, **a** E_{LOC} and **b** E_{Θ}

4 Discussion

Approximation of the load–displacement relationships of spinal motion segments by the proposed tangent function offered an improvement in in vivo characterization of the spine stiffness for patient-specific scoliotic spine models, compared to linear functions. The spine models characterized based on the tangent function yielded less discrepancy between the shapes of the simulated spines and X-rays than the models characterized based on the linear function (66, 55, and 39 % more accurate estimates of Ferguson angle, LOC, and Θ, respectively). The less discrepancy shows more accurate simulation of the patients' spine response to load, implying better estimates of the spine stiffness. In the following, through an example of Model-2 (linear approach) from our patient cohort, we describe in detail how the discrepancy can be related to the estimates of the stiffness. In the example (Fig. 5), the force is exerted on the model and it is increased from zero. In step 1, the model has bent as much as the measured lumbar spine according to the small discrepancy between the simulated and measured spines in the lumbar region, whereas it has bent less than the measured thoracic spine. By increasing the force (step 2), when T2 has reached its measured location, the model has bent more than the measured lumbar spine and
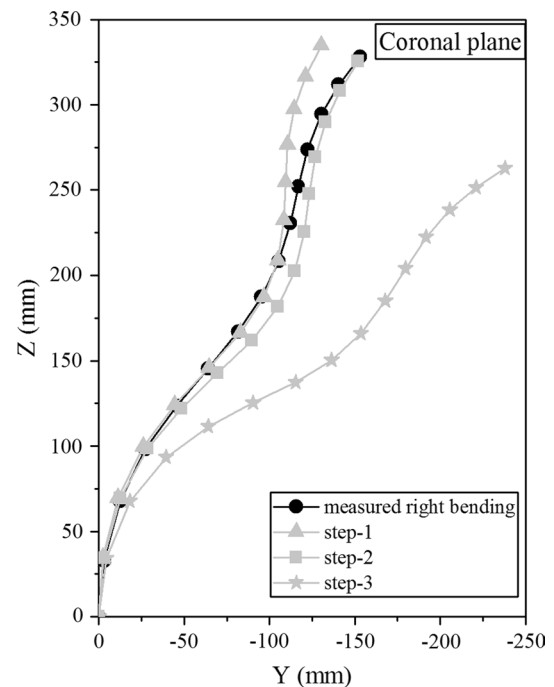

Fig. 5 Relation between the discrepancy (between the simulated and measured spines) and the estimates of the spine stiffness
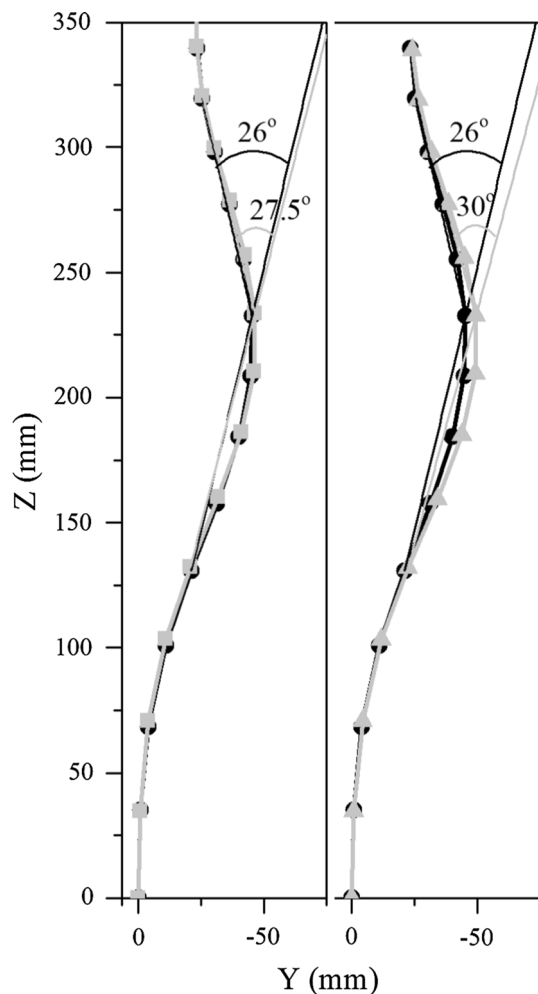
Fig. 6 Example of two simulations of the spine in the traction position and their estimated Ferguson angles; the *black colour* represents the measured spine, and the *grey colour* represents the simulated spines. E_{LOC} and E_{Θ} of the grey spine (*with square symbols*) in the *left side* are about 20 % smaller than those of the grey spine (*with triangle symbols*) in the *right side*

still it has not bent as much as the measured thoracic spine. By further increasing the force (step-3), the model has eventually bent as much as the measured thoracic spine, while the lumbar spine has bent much more than the measured lumbar spine. Therefore, in this example, the discrepancies can show the underestimation of the stiffness of the lumbar spine or overestimation of the stiffness of the thoracic spine.

The improvements offered by our method in estimation errors of LOC and Θ can have significant effects on reduction of the discrepancies between the simulated and measured spines. For example, Fig. 6 illustrates the simulated spines (the grey spines) with about 20 % difference in both

E_{LOC} and E_{Θ} (the left grey spine has 20 % smaller errors than the right grey spine). As can be seen, the enhancement of 20 % (almost half of the enhancement achieved by our method) can be influential to the fitting (the similarity between the spine curvatures) and estimates of Ferguson angle (error of 1.5° vs. 4°; 63 % smaller) as one of the important factors used to assess the similarity between the simulated and measured spines [5, 32].

The improvements were achieved because the proposed tangent function could deal with both infinitesimal and finite displacements and could limit the displacements as shown in Sect. 3.1. To further analyse the capability of the tangent function, we divided the displacements into three ranges, namely infinitesimal [0,0.2R), finite [0.2R,0.8R), and large finite [0.8R,R) and then studied the estimation errors of r in these ranges (Fig. 7). These ranges were considered because of the noticeable differences between $\Delta r/\Delta F$ in the ranges according to the experimental data in the literature [16, 30]. The estimation errors of r by the tangent functions were smaller than the errors by the linear functions in all the three ranges, 46, 32, and 45 % smaller errors for the infinitesimal, finite, and large finite ranges, respectively. Besides, a visual comparison (Fig. 7) also shows the effective reduction of the errors. The smaller errors can be attributed to the capability of the proposed tangent function for distinguishing the three ranges and making good estimates of $\Delta r/\Delta F$ associated with each range. In contrast, the linear function offered a constant $\Delta r/\Delta F$ over the whole displacement range and consequently induced larger errors. Overall, it can be concluded that the proposed tangent function is a good choice for approximation of the load–displacement relationships of the spinal motion segments.

In addition to the infinitesimal and finite ranges, the tangent function allows to deal with the situations in which the displacements are in the large finite range (Fig. 7). Simulation of scoliosis surgery is an example of such situations. In the surgery, surgeons try to straighten the spine curvature in the coronal plane by using spinal instrumentation and fusion that involve the large forces and moments according to [5, 35]. Therefore, our method, by better approximation of the displacements against the large loads, can improve the ability of biomechanical multi-body models in the surgery simulation as one of the potentially important applications of the models. The exploitation of such biomechanical models can provide clinicians with more accurate predictive information of spine correction under different surgery plans to propose a better plan.

Although the rotations measured on the lateral bending X-rays are mainly produced by the lateral bending of the spinal motion segments [32], they may be influenced by
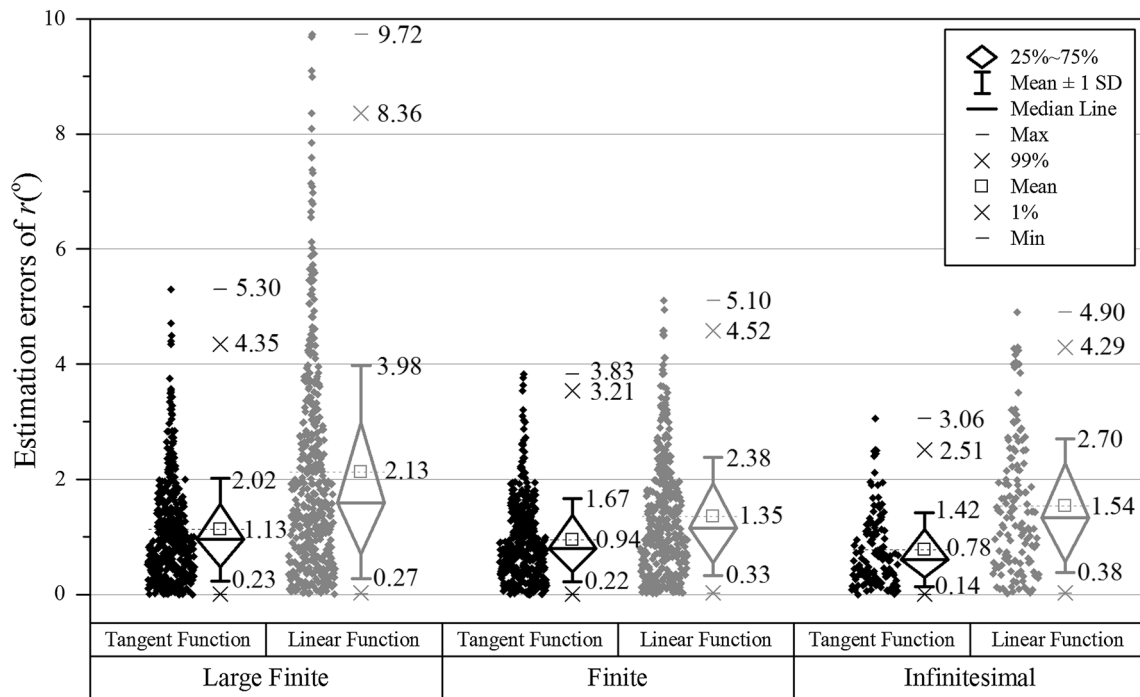
Fig. 7 The *box charts* of the estimation errors of *r* for the three ranges of the rotational displacements

the coupled motions. This can affect the asymptotes of the tangent functions and accordingly the estimated stiffness of the spinal motion segments. Analysis of the displacements in 3D can help disguising the motions for better characterization of the tangent function. Another factor that affects the asymptotes is the assumption made for setting *R* when the vertebrae rotate in the opposite direction of the bending movement. In this case, the estimation errors of *r* were $1.31 \pm 0.91°$ and $2.65 \pm 1.72°$ by Model-1 and Model-2, respectively. As is clear, both approximations by the tangent and linear functions resulted in larger mean values of errors than those in Fig. 7. However, the tangent function is superior to the linear function in this case as well, 51 % smaller errors by the tangent function.

The characterization of the spine stiffness was limited to the coronal plane in this study, as only 2D information was available from the X-rays. According to the experimental data of the other two planes (i.e. sagittal and transverse planes) reported in [28, 30], the load–displacement curves in these planes have almost similar characteristics as those we mentioned for the coronal plane in Sect. 2.2. Thus, our method could be extended to 3D planes and the consideration of the tangent function could be appropriate, once the patients' data of the two planes are available. Such an extension can lead to a more accurate estimation of the coupled motions, especially the more noticeable motions between the transverse and coronal planes. However, the

X-rays of the bending positions in the sagittal and transverse planes are not routine in scoliosis standard care, and thus, the extension of the method from 2D to 3D will require a more sophisticated measurement of the displacements in 3D.

5 Conclusions

This paper developed a method for nonlinear approximation of the load–displacement relationships of spinal motion segments to assist characterizing in vivo the stiffness of the scoliotic spine models. Tangent function was proposed to approximate the load–displacement relationships according to the characteristics of the load–displacement curves reported in the literature. To characterize the tangent function, lateral bending test was adopted. It was shown that the proposed tangent function could be superior to the linear function that is mainly used for the approximation of the load–displacement relationships. We demonstrated the higher capability of the tangent function to deal with a range of infinitesimal to large displacements involved in the spine movement to four positions (right bending, left bending, neutral, and traction).

The models developed based on the tangent functions resulted in more accurate estimates of Ferguson angles, locations of vertebrae, and orientations of vertebrae in the

four positions, in comparison with the models developed based on the linear functions. Besides, it was shown that the models developed based on the tangent functions simulated the neutral and traction positions, not included in the characterization of the tangent functions, as accurate as the bending positions included in the characterization. These results imply good estimates of the spine response to loads by the approximation using the proposed tangent function. Overall, we showed the ability of our method to assist characterizing in vivo the stiffness of the scoliotic spine models.

Appendix

Period of tangent functions is influential to the fitting of such a function to data. The catch is that the data may not show where the vertical asymptotes will fall precisely, and thus, the period cannot be identified directly. To estimate the asymptotes, the range of the available data on the horizontal axis is considered as the initial value for the period of the tangent, and then, both sides of the range are extended until the best fitting is achieved. In our case, the rotational displacements from the erect to right/left bending positions are considered as the initial value for the period. This traces back to the fact that the patients perform maximum voluntary bending movements to the right/left sides, implying that the vertebrae may rotate almost as much as their displacement limits (the vertical asymptotes). Therefore, to identify $R_{\text{Right/Left}}$, we studied the discrepancy between the fitted tangent functions and the displacement data acquired from the lateral bending X-rays against the extension to $[r_{\text{Right}}, r_{\text{Left}}]$ of the vertebrae (Fig. 8). To do the study, the minimization problem expressed by (5) was solved for 0, 10, 20, 30, and 40 % enlargements of $r_{\text{Right/Left}}$. According to RMSEs plotted in Fig. 8, the enlargement by 20 % resulted in the smallest discrepancies among the considered enlargement percentages. Therefore, $R_{\text{Right/Left}}$ was estimated by $1.2 \times r_{\text{Right/Left}}$.
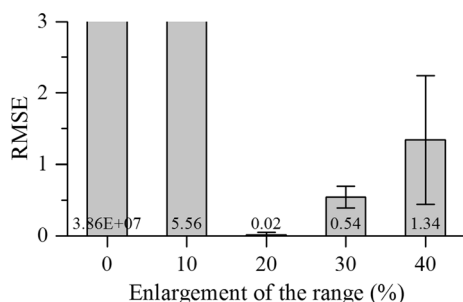
Fig. 8 The effect of enlargement of the range of the rotational displacements on the approximation of the load–displacement data by the tangent function

References

1. Abouhossein A, Weisse B, Ferguson SJ (2011) A multibody modelling approach to determine load sharing between passive elements of the lumbar spine. Comput Methods Biomech Biomed Eng 14:527–537
2. Asher MA, Burton DC (2006) Adolescent idiopathic scoliosis: natural history and long term treatment effects. Scoliosis 1:2
3. Ashton-Miller JA, Schultz AB (1987) Biomechanics of the human spine and trunk. Exerc Sport Sci Rev 16:169–204
4. Aubin C-E, Petit Y, Stokes I, Poulin F, Gardner-Morse M, Labelle H (2003) Biomechanical modeling of posterior instrumentation of the scoliotic spine. Comput Methods Biomech Biomed Eng 6:27–32
5. Aubin CE, Labelle H, Chevrefils C, Desroches G, Clin J, Eng ABM (2008) Preoperative planning simulator for spinal deformity surgeries. Spine 33:2143–2152
6. Bazrgari B, Shirazi-Adl A, Arjmand N (2007) Analysis of squat and stoop dynamic liftings: muscle forces and internal spinal loads. Eur Spine J 16:687–699
7. Chalmers E, Westover L, Jacob J, Donauer A, Zhao V, Parent E, Moreau M, Mahood J, Hedden D, Lou EM (2015) Predicting success or failure of brace treatment for adolescents with idiopathic scoliosis. Med Biol Eng Computt 53:1001–1009. doi:10.1007/s11517-015-1306-7
8. Cheriet F, Meunier J (1999) Self-calibration of a biplane X-ray imaging system for an optimal three dimensional reconstruction. Comput Med Imaging Graph 23:133–141
9. Christophy M, Curtin M, Senan NAF, Lotz JC, O'Reilly OM (2013) On the modeling of the intervertebral joint in multibody models for the spine. Multibody SysDyn 30:413–432
10. Christophy M, Senan NAF, Lotz JC, O'Reilly OM (2012) A musculoskeletal model for the lumbar spine. Biomech Model Mechanobiol 11:19–34
11. Colton T (1974) Statistics in medicine. Little, Brown, Boston, p 164
12. Desroches G, Aubin C-E, Sucato DJ, Rivard C-H (2007) Simulation of an anterior spine instrumentation in adolescent idiopathic scoliosis using a flexible multi-body model. Med Biol Eng Comput 45:759–768
13. Duke K, Aubin C-E, Dansereau J, Labelle H (2005) Biomechanical simulations of scoliotic spine correction due to prone position and anaesthesia prior to surgical instrumentation. Clin Biomech 20:923–931
14. Engsberg JR, Lenke LG, Reitenbach AK, Hollander KW, Bridwell KH, Blanke K (2002) Prospective evaluation of trunk range of motion in adolescents with idiopathic scoliosis undergoing spinal fusion surgery. Spine 27:1346–1354
15. Gardner-Morse MG, Stokes IA (2004) Structural behavior of human lumbar spinal motion segments. J Biomech 37:205–212
16. Heuer F, Schmidt H, Klezl Z, Claes L, Wilke H-J (2007) Stepwise reduction of functional spinal structures increase range of motion and change lordosis angle. J Biomech 40:271–280
17. Huynh K, Gibson I, Jagdish B, Lu W (2015) Development and validation of a discretised multi-body spine model in LifeMOD for biodynamic behaviour simulation. Comput Methods Biomech Biomed Eng 18:175–184
18. Jalalian A, Gibson I, Tay EH (2013) Computational biomechanical modeling of scoliotic spine: challenges and opportunities. Spine Deform 1:401–411
19. Jalalian A, Tay EH, Arastehfar S, Gibson I, Liu G (2016) Finding line of action of the force exerted on erect spine based on lateral bending test in personalization of scoliotic spine models. Med Biol Eng Comput. doi:10.1007/s11517-016-1550-5

20 Jalalian A, Tay EH, Arastehfar S, Liu G (2016) A patient-specific multibody kinematic model for representation of the scoliotic spine movement in frontal plane of the human body. Multibody Syst Dyn

21 Jalalian A, Tay EH, Liu G (2016) Data mining in medicine: relationship of scoliotic spine curvature to the movement sequence of lateral bending positions. In: 15th industrial conference on data mining ICDM 2016, New York, USA, 12–14 July 2016. Springer International Publishing, pp 29–40

22 Jalalian A, Tay EH, Liu G A hypothesis about line of action of the force exerted on spine based on lateral bending test in personalized scoliotic spine models. In: The Canadian society for mechanical engineering international congress, Kelowna, BC, Canada, June 26–29, 2016

23 Keenan BE, Izatt MT, Askin GN, Labrom RD, Pettet GJ, Pearcy MJ, Adam CJ (2014) Segmental torso masses in adolescent idiopathic scoliosis. Clin Biomech 29:773–779

24 Klepps SJ, Lenke LG, Bridwell KH, Bassett GS, Whorton J (2001) Prospective comparison of flexibility radiographs in adolescent idiopathic scoliosis. Spine 26:E74–E79

25 Little JP, Adam C (2011) Patient-specific computational biomechanics for simulating adolescent scoliosis surgery: predicted vs clinical correction for a preliminary series of six patients. Int J Numer Methods Biomed Eng 27:347–356

26 McGill SM, Norman RW (1987) Effects of an anatomically detailed erector spinae model on L4L5 disc compression and shear. J Biomech 20:591–600

27 O'Reilly OM, Metzger MF, Buckley JM, Moody DA, Lotz JC (2009) On the stiffness matrix of the intervertebral joint: application to total disk replacement. J Biomech Eng 131:081007

28 Oxland TR, Lin RM, Panjabi MM (1992) Three-dimensional mechanical properties of the thoracolumbar junction. J Orthop Res 10:573–580

29 Panjabi MM, Brand RA Jr, White AA III (1976) Three-dimensional flexibility and stiffness properties of the human thoracic spine. J Biomech 9:185–192

30 Panjabi MM, Oxland T, Yamamoto I, Crisco J (1994) Mechanical behavior of the human lumbar and lumbosacral spine as shown by three-dimensional load-displacement curves. J Bone Joint Surg 76:413–424

31 Perret C, Poiraudeau S, Fermanian J, Revel M (2001) Pelvic mobility when bending forward in standing position: validity and reliability of 2 motion analysis devices. Arch Phys Med Rehabil 82:221–226

32 Petit Y, Aubin C, Labelle H (2004) Patient-specific mechanical properties of a flexible multi-body model of the scoliotic spine. Med Biol Eng Comput 42:55–60

33 Polly DW Jr, Sturm PF (1998) Traction versus supine side bending: which technique best determines curve flexibility? Spine 23:804–808

34 Rupp T, Ehlers W, Karajan N, Günther M, Schmitt S (2015) A forward dynamics simulation of human lumbar spine flexion predicting the load sharing of intervertebral discs, ligaments, and muscles. Biomech Model Mechanobiol 14:1081–1105

35 Salmingo RA, Tadano S, Fujisaki K, Abe Y, Ito M (2013) Relationship of forces acting on implant rods and degree of scoliosis correction. Clin Biomech 28:122–128

36 Shojaei I, Arjmand N, Bazrgari B (2015) An optimization-based method for prediction of lumbar spine segmental kinematics from the measurements of thorax and pelvic kinematics. Int J Numer Methods Biomed Eng 31(12). doi:10.1002/cnm.2729

37 Stokes I, Iatridis J (2005) Biomechanics of the spine. In: Mow VC, Huiskes R (eds) Basic orthopaedic biomechanics and mechano-biology. Lippincott Williams, Wilkins, Philadelphia, pp 196–197

38 Stokes IA (1994) Three-dimensional terminology of spinal deformity: a report presented to the scoliosis research society by the scoliosis research society working group on 3-D terminology of spinal deformity. Spine 19:236–248

39 Stokes IA, Gardner-Morse M, Churchill D, Laible JP (2002) Measurement of a spinal motion segment stiffness matrix. J Biomech 35:517–521

40 Three-Dimensional Terminology of Spinal Deformity (2001) Scoliosis research society. http://www.srs.org/professionals/glossary/SRS_3D_terminology.htm-1. Accessed 29 Dec 2014

41 Udoekwere UI, Krzak JJ, Graf A, Hassani S, Tarima S, Riordan M, Sturm PF, Hammerberg KW, Gupta P, Anissipour AK (2014) Effect of lowest instrumented vertebra on trunk mobility in patients with adolescent idiopathic scoliosis undergoing a posterior spinal fusion. Spine Deformity 2:291–300

42 Wagnac E, Arnoux P-J, Garo A, Aubin C-E (2012) Finite element analysis of the influence of loading rate on a model of the full lumbar spine under dynamic loading conditions. Med Biol Eng Comput 50:903–915. doi:10.1007/s11517-012-0908-6

43 Wong KW, Leong JC, M-k Chan, Luk KD, Lu WW (2004) The flexion–extension profile of lumbar spine in 100 healthy volunteers. Spine 29:1636–1641

Athena Jalalian is working on computational biomechanical multi-body modelling of scoliotic spine for surgical correction prediction. She particularly focuses on personalization of mechanical properties of multi-body models.

Francis E. H. Tay has conducted extensive research into computational biomechanical multi-body models of scoliotic spine. His research area includes rehabilitation and scoliosis.

Soheil Arastehfar is a research fellow at National University of Singapore. His research interests are multibody system dynamics, mechanism design, and robotics.

Gabriel Liu is the head and senior consultant of the university spine centre, Department of Orthopaedic Surgery at National University of Singapore. He is interested in research into scoliosis surgery planning by using computational biomechanical models.